

FULL IN-PLANE SEPARATION OF RESPONSE FUNCTIONS AND THE STUDY OF TWO-BODY SHORT RANGE CORRELATIONS VIA THE $^{16}\text{O}(e,e'p)$ REACTION.

A. Saha, J. Mougey, J. LeRose, S. Nanda, P. Ulmer, CEBAF; L. Chinitz, R. Minehart, University of Virginia; M. Bernheim, M. Brussel, J.F. Danel, L. Lakahal-Ayat, J.M. LeGoff, A. Magnon, C. Marchand, J. Morgenstern, J. Picard, P. Vernin CEN-Saclay; G. Capitani, E. De Sanctis, INFN-LNF, Frascati; A. Catarinella, S. Frulani, F. Garibaldi, F. Ghio, M. Iodice, INFN-ISS, Rome; C. Perdrisat, College of William and Mary; V. Punjabi, Norfolk State University; R. Powers, University of Basel.

In one of the first measurements of its kind, the nuclear interference response function R_{LT} has been determined in a coincidence $(e,e'p)$ experiment on ^{16}O for the ground state ($p_{1/2}$) and the first excited state ($p_{3/2}$) of the residual ^{15}N nucleus. The experiment has been performed at SACLAY with a waterfall target. Figure 1 shows a representative spectrum.

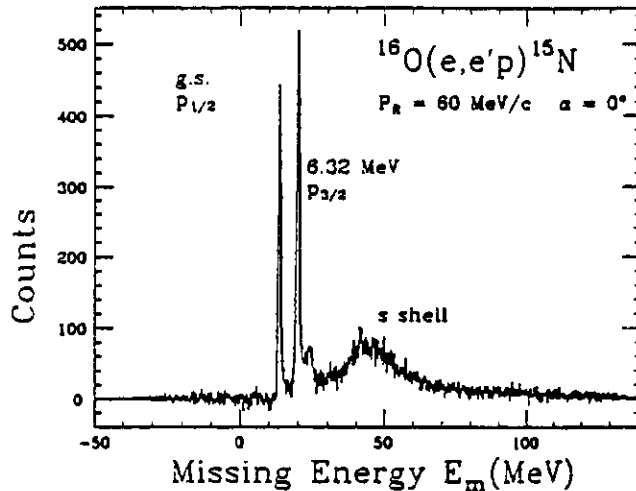


Figure 1. Missing Energy Spectrum for the $^{16}\text{O}(e,e'p)$ reaction performed at $E_0 = 580$ MeV and $T_p = 160$ MeV. The momentum transfer is $\vec{q} = 570$ MeV/c and the recoil momentum is $p_R = 60$ MeV/c.

In general, the $(e,e'p)$ cross section can be expressed in terms of four response functions R_L , R_T , R_{LT} and R_{TT} ^[1,2]. With three in-plane kinematics, two with electrons scattered in the forward direction and one in the backward direction, we are able to separate R_T , R_{LT} and $R_L + R_{TT}$. In order to separate R_L and R_{TT} , the proton has to be detected out of the scattering plane.

With a beam energy of 580 MeV, we performed the two measurements at forward kinematics, with coincident protons measured on either side of \vec{q} . This allows determination of R_{LT} which is proportional to the difference in the cross sections in the two kinematics. Results of these forward kinematics are presented here. Recently, the backward kinematics measurement was also completed at Saclay with an incident beam energy of 398 MeV and

the analysis of this data is currently underway and shall be presented elsewhere. In all three kinematical setups, perpendicular kinematics was employed, where the momentum transfer $\vec{q} = 570 \text{ MeV}/c$ and the center of mass energy $e_{cm} = 149 \text{ MeV}$ of the final system were kept constant. The outgoing proton energy was kept fixed at $T_p = 160 \text{ MeV}$.

In PWIA, the cross section can be factorized into two parts, a dynamical term $K\sigma_{ep}$ representing the off-shell electron-proton interaction, and a nuclear structure term $S_F(E_m, p_R)$ called the spectral function. In our analysis we used the CC1 prescription of DeForest^[1] for $K\sigma_{ep}$. When the measured cross section is divided by $K\sigma_{ep}$ we obtain the so called "effective spectral function". Integration of the spectral function over all momenta and energy of a given shell gives the spectroscopic factor for that shell. In a naïve shell model this factor should be $2j + 1$ for a full shell, where j is the total angular momentum of the proton for that shell.

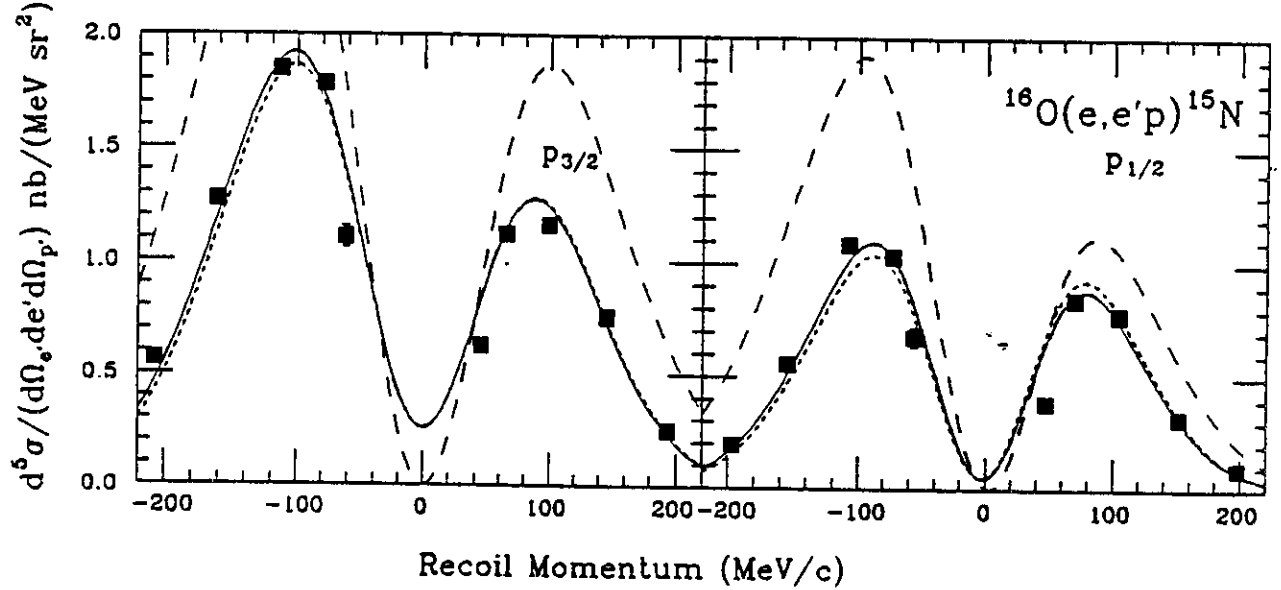


Figure 2 Cross section for the $p_{1/2}$ and the $p_{3/2}$ states shown as functions of the recoil momentum p_R . The solid curves are relativistic DWIA calculations, the short-dashed curves are non-relativistic DWIA calculations and the long-dashed curves are relativistic PWIA calculations. The calculations are from Van Orden^[2].

In figure 2 the reaction cross section as a function of p_R for both the g.s. ($p_{1/2}$) and the 6.32 MeV ($p_{3/2}$) state is shown. The effective spectral function $S_F = \frac{d^5\sigma}{K\sigma_{ep}}$, and the interference response function R_{LT} are shown in figures 3 and 4 respectively. Figure 5 shows the ratio of the cross sections in the two kinematic regions (protons detected forward ($\alpha = 0^\circ$) and backward ($\alpha = 180^\circ$) of \vec{q} respectively) divided by the corresponding DeForest CC1 σ_{ep} cross sections. The data have been corrected for radiative effects. The error bars shown statistical only.

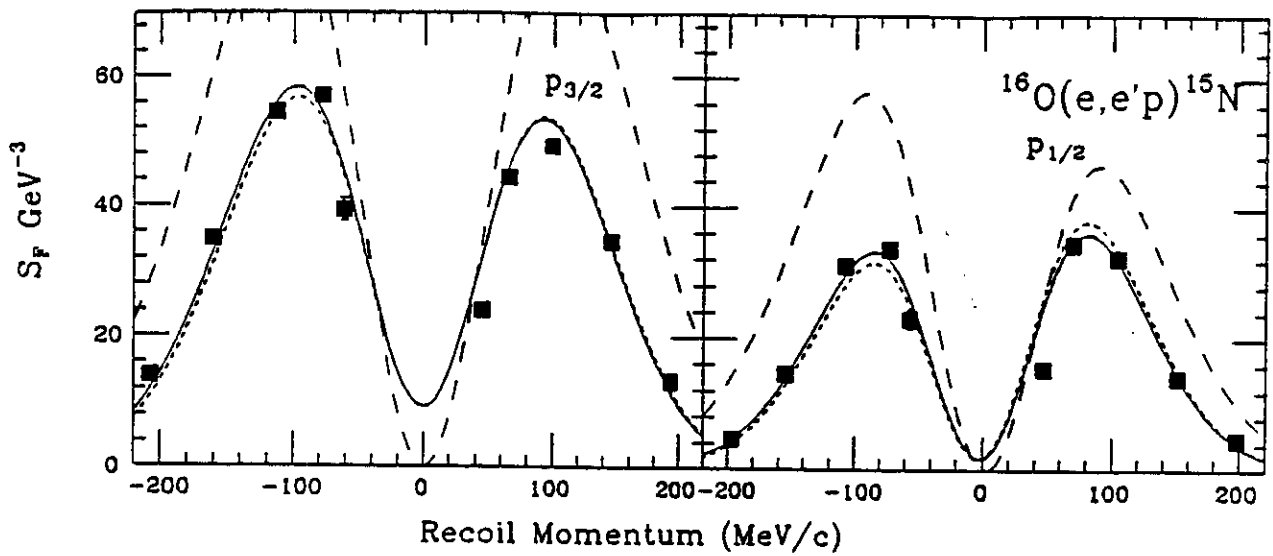


Figure 3 Spectral functions for the $p_{1/2}$ and the $p_{3/2}$ states. The curves are the same as for figure 2.

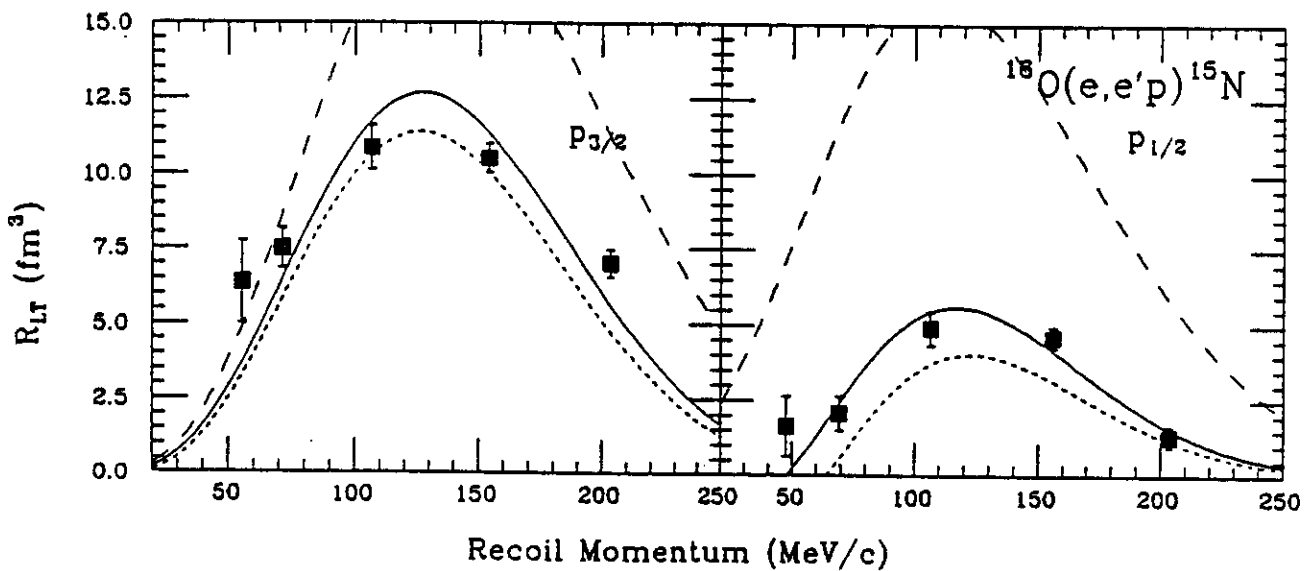


Figure 4 Interference Response Functions R_{LT} for the $p_{1/2}$ and the $p_{3/2}$ states. The curves are the same as for figure 2.

Fully relativistic DWIA calculations (solid curves in figures 2 to 5) have been performed by Van Orden^[2] using Dirac distorted waves for the ejected proton and Dirac-Hartree wave functions for the bound state. A non-relativistic reduction is also presented (short-dashed curves) as well as a relativistic PWIA calculation (long-dashed curves). In

at the 50% level.

In another part of the $^{16}\text{O}(e,e'p)$ experiment we chose specific kinematic regions to study the high momentum components of the nucleon wave functions. These studies are of special interest as they are sensitive to correlations arising from the short range part of the nucleon-nucleon interaction. Self consistent mean field descriptions of nuclei fail to describe these components and significant non-nucleonic degrees of freedom (MEC, IC) are necessary to adequately explain the existing data for $\text{D}^{[5,6]}$ and $^3\text{He}^{[7]}$ at high values of recoil momenta ($p_R \sim 500 \text{ MeV}/c$). Moreover, since short range correlations reflect short distance behaviour, they could in principle also reflect sub-nucleonic degrees of freedom. Calculations by Ciofi degli Atti *et al*^[8] in ^3He show a definite relationship between high-momentum components and continuum strength. The proton momentum distributions obtained by integrating the one-body spectral function $S(\vec{p}, E_m)$ over missing energy, E_m , show that the high momentum strength is completely dominated by correlations and that it is spread over a large continuum in missing energy.

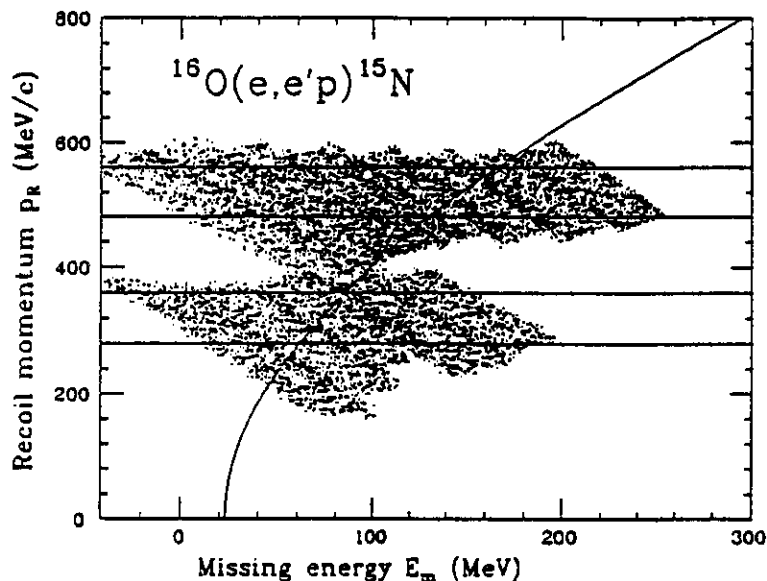


Figure 6. Scatter plot showing the phase space covered in the $^{16}\text{O}(e,e'p)$ reaction for the various kinematical domains centered around $p_R = 320 \text{ MeV}/c$ and $p_R = 520 \text{ MeV}/c$. The solid line indicates the kinematics expected from an interaction with a two-nucleon pair in ^{16}O .

Measurements were taken at an incident energy of 590 MeV in two sets of kinematics, one centered at $p_R=320 \text{ MeV}/c$ spanning missing energies from $E_m = 0$ to 180 MeV and the other at $p_R=520 \text{ MeV}/c$ from $E_m = 0$ to 240 MeV (see figure 6). Figure 7 shows the two data points integrated over the missing energy range in the two p_R regions. These results are very preliminary.

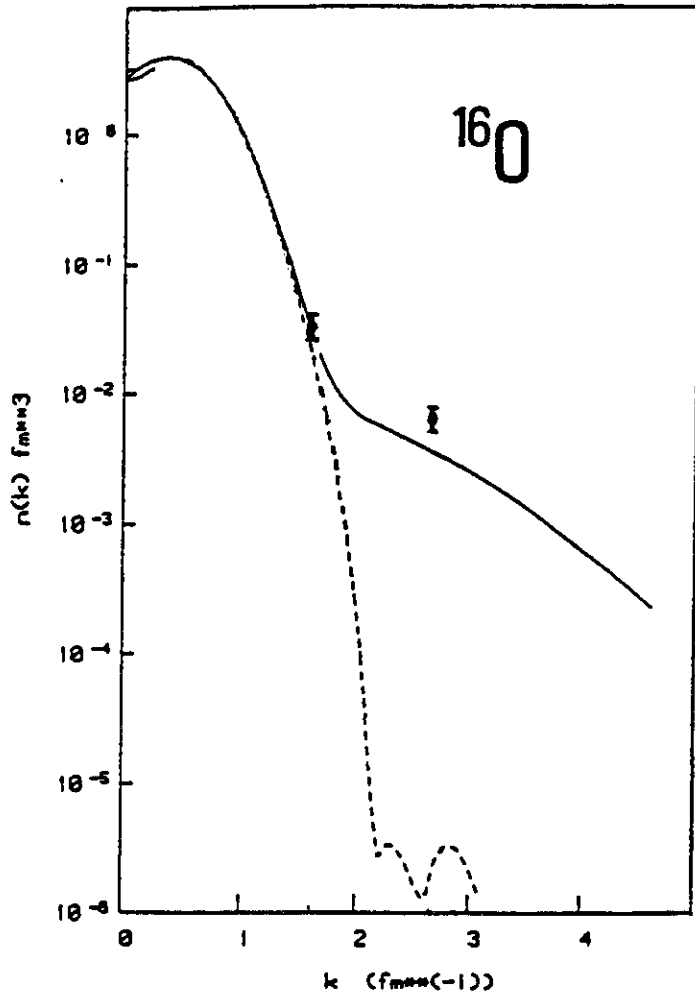


Figure 7. Nucleon momentum distributions in ^{16}O . The data points are from the present experiment. The full curves are correlated nucleon momentum distributions calculated within a many body approach and using a realistic nucleon-nucleon interaction^[8]. The dashed curve is a calculation using a density-dependent HF wave function^[9].

References

- [1] T. DeForest Jr., Nucl. Phys. A392, 232 (1983).
- [2] A. Picklesimer and J.W. van Orden, Phys. Rev. C40, 290 (1989). J.W. van Orden, priv. comm. (1990).
- [3] E.J. Moniz *et al*, Phys. Rev. Lett. 26, 445 (1971). P. Barreau *et al*, Nucl. Phys. A402, 515 (1983) R. Altemus *et al*, Phys. Rev. Lett. 41, 965 (1980). Z.E. Meziani *et al*, Phys. Rev. Lett 52, 2130 (1984), 54, 1233 (1985). C. Marchand *et al*, Phys. Lett. 153B, 29 (1985)
- [4] P. E. Ulmer *et al*, Phys. Rev. Lett. 59, 2259 (1987) A. Magnon *et al*, Phys. Lett. 222B, 352 (1989). D. Reffay-Pikeroen *et al*, Phys. Rev. Lett. 60, 776 (1988).
- [5] S. Turck-Chieze *et al*, Phys. Lett. 142B, 145 (1984).
- [6] M. Bernheim *et al*, Nucl. Phys. A365, 349 (1981).
- [7] C. Marchand *et al*, Phys. Rev. Lett. 60, 1703 (1988).
- [8] C. Ciofi degli Atti *et al*, Phys. Lett. A449, 219 (1986).
- [9] J. Carlson and M.H. Kalos, Phys. Rev. C32, 2105 (1985).